Interelectronic-interaction effect on the radiative recombination of an electron with a heavy He-like ion

V. A. Yerokhin,[1,2] V. M. Shabaev,[1,3] T. Beier,[4] and J. Eichler[1]
[1]*Bereich Theoretische Physik, Hahn-Meitner-Institut, 14109 Berlin, Germany*
[2]*Institute for High Performance Computing and Data Bases, Fontanka 118, St. Petersburg 198005, Russia*
[3]*Department of Physics, St. Petersburg State University, Oulianovskaya 1, Petrodvorets, St. Petersburg 198904, Russia*
[4]*Fysik och Teknisk Fysik, Chalmers Tekniska Högskola och Göteborgs Universitet, SE-412 96 Göteborg, Sweden*
(Received 5 April 2000; published 19 September 2000)

Interelectronic-interaction correction of first order in $1/Z$ is studied for radiative recombination of an electron with a heavy He-like ion in the ground state. A rigorous relativistic treatment is compared with two frequently applied approximations. A calculation is carried out for radiative recombination of an electron into $2s$, $2p_{1/2}$, and $2p_{3/2}$ states of He-like uranium for impact energies between 10 and 700 MeV/u.

PACS number(s): 34.80.Lx, 31.30.Jv, 34.10.+x, 34.70.+e

I. INTRODUCTION

In energetic atomic collisions between highly charged high-Z ions and low-Z target atoms, radiative electron capture (REC) is one of the most important reaction channels. In the limit of a loosely bound target electron, REC is identical with radiative recombination or its time-reversed analog, the photoionization process. Reactions of this type have been extensively studied in recent years for heavy highly charged projectiles up to bare uranium. The relativistic theory of REC in the one-electron approximation is well established at present (see Ref. [1] and references therein), and results of numerical calculations [2] are in excellent agreement with experiments. In particular, the spin-flip contribution to REC, calculated in Ref. [2], was recently identified in angular-differential measurements [3].

While radiative recombination of an electron with a bare nucleus is well understood theoretically, the process involving an ion with several electrons is complicated by the interelectronic interaction. The REC process into the L-shell of He-like uranium was studied both experimentally and theoretically in Ref. [4]. In that work, the interelectronic interaction was taken into account using a simple model employing an effective nuclear charge of $Z_{\rm eff}=90.3$. On the level of the experimental accuracy, this model provides a satisfactory description of the process. However, in view of the progress in experimental techniques that has been achieved during the last few years, it is tempting to search for a rigorous theoretical description of interelectronic-interaction effects in these processes. A systematic QED theory of radiative recombination has been worked out in Refs. [5,6]. In the present work, we apply this theory to a rigorous investigation of the interelectronic-interaction corrections of first order in $1/Z$ to radiative recombination of an electron with a helium-like ion. Our treatment is exact in this order, i.e., the full photon propagator is used, including the Coulomb, Breit, and retarded parts.

Relativistic units ($\hbar=c=1$) are used in the article.

II. BASIC FORMULAS

We consider radiative recombination of an electron with momentum $\mathbf{p}_i$ and polarization μ_i with a heavy He-like atom in the ground state that is placed at the origin of the coordinate frame. The final state of the system is a Li-like ion in the state $(1s)^2 v$, where v denotes a valence electron. This picture corresponds to the projectile system, if we study the radiative recombination of a free target electron with a heavy He-like projectile. The differential cross section of this process is given by

$$d\sigma=\frac{(2\pi)^4}{v_i}|\tau|^2\,\delta(E_{\rm f}+k_f^0-E_{\rm i}-p_i^0)\,d\mathbf{k}_f, \tag{1}$$

where $E_{\rm i}$ and $E_{\rm f}$ are the energies of the initial ($|{\rm i}\rangle$) and the final ($|{\rm f}\rangle$) states of the atom, respectively; $p_i^0=\sqrt{\mathbf{p}_i^2+m^2}$ is the energy of the incident electron, $k_f=(k_f^0,\mathbf{k}_f)$ where k_f^0 and $\mathbf{k}_f$ are the photon energy and momentum, respectively; v_i is the velocity of the incident electron in the projectile frame, and τ is the amplitude of the process that is connected to the S-matrix element by

$$\langle k_f\epsilon_f,{\rm f}|S|p_i\mu_i,{\rm i}\rangle=2\pi i\,\delta(E_{\rm f}+k_f^0-E_{\rm i}-p_i^0)\,\tau. \tag{2}$$

Here $\epsilon_f=(0,\boldsymbol{\epsilon}_f)$ is the photon polarization and $p_i=(p_i^0,\mathbf{p}_i)$. To zeroth order the amplitude of the process is given by (see, e.g., Ref. [6])

$$\tau^{(0)}=\langle v|e\,\boldsymbol{\alpha}\cdot\mathbf{A}_f^*|p\rangle, \tag{3}$$

where $|v\rangle$ denotes the wave function of the valence electron,

$$\mathbf{A}_f(\mathbf{x})=\frac{\boldsymbol{\epsilon}_f\exp(i\mathbf{k}_f\cdot\mathbf{x})}{\sqrt{2k_f^0(2\pi)^3}} \tag{4}$$

is the wave function of the photon, and $|p\rangle=\psi_{p_i\mu_i(+)}(\mathbf{x})$ indicates the wave function of the incoming electron in the continuum spectrum with a defined asymptotic momentum, defined by

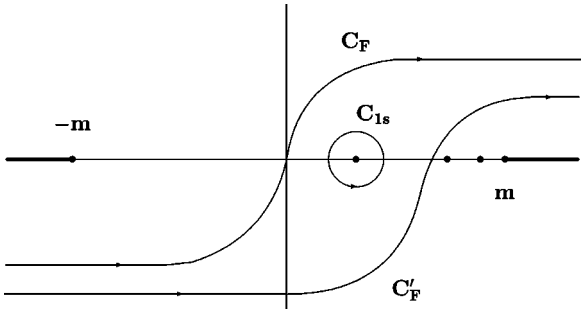

FIG. 1. The branch cuts and the poles of the Dirac-Coulomb Green function in the complex energy plane. C_F indicates the Feynman integration contour for the standard vacuum; C_F' denotes the integration contour for the vacuum with the $(1s)^2$-shell included.

$$\psi_{p_i\mu_i(+)}=\frac{u(p_i,\mu_i)\exp(i\mathbf{p}_i\cdot\mathbf{x})}{\sqrt{\frac{p_i^0}{m}(2\pi)^3}} +[p_i^0-H_0(1-i0)]^{-1}V_C\psi_{p_i\mu_i(+)}. \quad (5)$$

Here $H_0=\boldsymbol{\alpha}\cdot\mathbf{p}+\beta m$ is the free-electron Hamiltonian, V_C indicates the nuclear potential, and $\overline{u}u=1$. To zeroth order the process considered here is equivalent to the capture of an electron by a bare nucleus.

The derivation of expressions for interelectronic-interaction corrections can be simplified significantly because we consider the radiative recombination of an electron with an atom in a closed-shell configuration. As is known (see, e.g., Ref. [7]), closed shells can be taken into account simply by a redefinition of the vacuum. In our case, we regard the $(1s)^2$-shell as belonging to a new vacuum. This redefinition of the vacuum corresponds to a replacement of the standard Feynman integration contour (indicated by C_F in Fig. 1) by a new contour denoted by C_F' in Fig. 1. The one-electron corrections calculated with the new vacuum include the whole effect of an interaction with the $(1s)^2$-shell. Therefore, the interelectronic-interaction correction can be found as the difference of the one-electron corrections calculated with the new vacuum and with the standard one. The difference of integrals along the contours C_F and C_F' is an integral along the contour C_{1s}, i.e., the pole contribution at the point $\omega=\varepsilon_{1s}$. This is illustrated in Fig. 1. QED corrections of first order in α for radiative recombination of an electron with a bare nucleus were recently derived in Ref. [6]. A simple recipe can be given to obtain general expressions for the interelectronic-interaction corrections of first order in $1/Z$ from the corresponding expressions for the QED corrections in Ref. [6]. All energy integrations along the standard Feynman contour C_F should be replaced by a pole contribution at the point $\omega=\varepsilon_{1s}$. We note that, unlike the QED corrections, the pole contribution is free from ultraviolet and infrared divergences.

The derivation as described above yields to first order in $1/Z$,

$$\tau_{\rm int}^{(1)}=\sum_{l=1}^{4}\tau_l^{\rm int}, \quad (6)$$

where

$$\tau_1^{\rm int}=\sum_{\mu_c}\sum_P(-1)^P \times\sum_{\varepsilon_n\neq\varepsilon_v}\frac{\langle PvPc|I(\Delta_{Pcc})|nc\rangle\langle n|e\boldsymbol{\alpha}\cdot\mathbf{A}_f^*|p\rangle}{\varepsilon_v-\varepsilon_n} +\sum_{\mu_c}\left(-\frac{1}{2}\right)\langle cv|I'(\Delta_{vc})|vc\rangle\langle v|e\boldsymbol{\alpha}\cdot\mathbf{A}_f^*|p\rangle, \quad (7)$$

$$\tau_2^{\rm int}=\sum_{\mu_c}\sum_P(-1)^P\sum_n\frac{\langle v|e\boldsymbol{\alpha}\cdot\mathbf{A}_f^*|n\rangle\langle nc|I(\Delta_{Pcc})|PpPc\rangle}{p_i^0-\varepsilon_n(1-i0)}, \quad (8)$$

$$\tau_3^{\rm int}=\sum_{\mu_c}\sum_P(-1)^P\sum_n\frac{\langle PvPc|I(\Delta_{pPv})|pn\rangle\langle n|e\boldsymbol{\alpha}\cdot\mathbf{A}_f^*|c\rangle}{\varepsilon_c-k_f^0-\varepsilon_n(1-i0)}, \quad (9)$$

$$\tau_4^{\rm int}=\sum_{\mu_c}\sum_P(-1)^P\sum_n\frac{\langle c|e\boldsymbol{\alpha}\cdot\mathbf{A}_f^*|n\rangle\langle vn|I(\Delta_{Ppv})|PpPc\rangle}{\varepsilon_c+k_f^0-\varepsilon_n(1-i0)}. \quad (10)$$

Here, $|c\rangle=|\kappa_c\mu_c\rangle$ and $|v\rangle=|\kappa_v\mu_v\rangle$ are the wave functions of the core and the valence electrons, respectively; κ is the Dirac angular-momentum quantum number, μ indicates the momentum projection, the n-summation is performed over the whole spectrum of the Dirac equation, P is the permutation operator $[PaPb=(ab)$ or $(ba)]$, $\Delta_{ab}=\varepsilon_a-\varepsilon_b$, and $k_f^0=p_i^0-\varepsilon_v$ is the energy of the emitted photon. The other notations are $I'(\Delta)=[dI(\omega)/d\omega]_{\omega=\Delta}$,

$$I(\omega,\mathbf{x}_1,\mathbf{x}_2)=e^2\alpha_\mu\alpha_\nu D^{\mu\nu}(\omega,\mathbf{x}_1,\mathbf{x}_2) \quad (11)$$

is the operator of the interelectronic interaction, $\alpha_\mu=(1,\boldsymbol{\alpha})$ are the Dirac matrices,

$$D_{\mu\nu}(\omega,\mathbf{x}_1,\mathbf{x}_2)=g_{\mu\nu}\frac{\exp[i\sqrt{\omega^2+i\delta}|\mathbf{x}_1-\mathbf{x}_2|]}{4\pi|\mathbf{x}_1-\mathbf{x}_2|} \quad (12)$$

is the photon propagator in the Feynman gauge, the branch of the square root is fixed by the condition $\mathrm{Im}(\sqrt{\omega^2+i\delta})>0$, and δ is small and positive.

The corresponding Feynman diagrams are presented in Fig. 2. The diagrams Figs. 2(a) and 2(c) correspond to the *direct* $(PaPb=ab)$ and the *exchange* $(PaPb=ba)$ parts of $\tau_1^{\rm int}$, and the diagrams Figs. 2[(b),(d)], Figs. 2[(e),(g)], and Figs. 2[(f),(h)] correspond to the direct and the exchange parts of the corrections $\tau_2^{\rm int}$, $\tau_3^{\rm int}$, and $\tau_4^{\rm int}$, respectively.

Equations (7)–(10) represent the interelectronic-interaction corrections to the amplitude of the process. The corresponding corrections to the differential cross section are

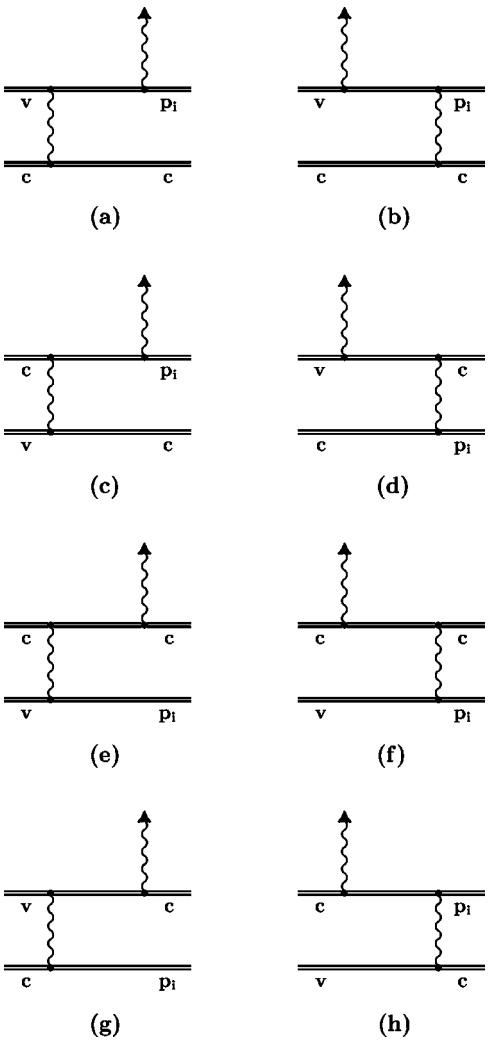

FIG. 2. Feynman diagrams representing the interelectronic-interaction corrections of first order in $1/Z$ to radiative recombination of an electron with a He-like atom; p_i denotes the incoming electron in the continuum spectrum, and v and c indicate the valence and the core electrons, respectively.

$$\frac{d\sigma_l^{\rm int}}{d\Omega_f}=\frac{(2\pi)^4}{v_i}\mathbf{k}_f^2 2\,{\rm Re}[\tau^{(0)*}\tau_l^{\rm int}]. \tag{13}$$

In addition to this, one should take into account a contribution originating from a modification of the energy of the emitted photon in the zeroth-order cross section due to the interelectronic interaction, given by

$$\frac{d\sigma_{\rm en}^{\rm int}}{d\Omega_f}=\left.\frac{d\sigma^{(0)}}{d\Omega_f}\right|_{k_f^0=p_i^0-\tilde{\varepsilon}_v}-\left.\frac{d\sigma^{(0)}}{d\Omega_f}\right|_{k_f^0=p_i^0-\varepsilon_v^{(0)}}. \tag{14}$$

Here $\tilde{\varepsilon}_v=\varepsilon_v^{(0)}+\Delta\varepsilon_{\rm int}^{(1)}$ is the energy of the valence electron including the first-order interelectronic-interaction correction,

$$\Delta\varepsilon_{\rm int}^{(1)}=\sum_{\mu_c}\sum_P(-1)^P\langle PvPc|I(\Delta_{Pv})|vc\rangle. \tag{15}$$

The total interelectronic-interaction correction to the cross section in first order in $1/Z$ is given by

$$\frac{d\sigma_{\rm int}^{(1)}}{d\Omega_f}=\frac{d\sigma_{\rm en}^{\rm int}}{d\Omega_f}+\sum_{l=1}^{4}\frac{d\sigma_l^{\rm int}}{d\Omega_f}. \tag{16}$$

We note that the direct part of the corrections $\tau_1^{\rm int}$ and $\tau_2^{\rm int}$ [diagrams Figs. 2(a) and 2(b)] has a transparent physical meaning. It can be shown that this part of the corrections corresponds to a modification of the incoming and the outgoing electron wave functions by the screening potential

$$V_{\rm scr}(x)=2\alpha\left\{\frac{1}{x}\int_0^x dy y^2[g_{1s}^2(y)+f_{1s}^2(y)]+\int_x^\infty dy y[g_{1s}^2(y)+f_{1s}^2(y)]\right\}, \tag{17}$$

where g_{1s} and f_{1s} are the upper and the lower components of the radial wave function of the ground state, respectively. From physical reasons, one can expect that the effect of the interelectronic interaction can be described with reasonable accuracy by considering the capture of an electron by a bare nucleus with the nuclear potential modified by the screening potential [Eq. (17)]. We refer to this approach as the *screening-potential* approximation. As we will show below, this simple approximation yields the dominant part of the interelectronic-interaction effect in a wide region of projectile energies.

We note that a resonance arises in Eq. (10) when the energy argument of the Green function comes close to a discrete energy level

$$p_i^0-(\varepsilon_v-\varepsilon_c)\approx\varepsilon_n. \tag{18}$$

This corresponds to the resonant process of dielectronic recombination. As it stands, Eq. (10) is valid only in the nonresonant case. Resonant processes can be rigorously treated by the method developed in Ref. [5]. In this article we study only the nonresonant process of radiative recombination and exclude from the consideration energy intervals close to the resonances [Eq. (18)]. For the states under consideration, these resonances occur in the region of projectile energies of 115–190 MeV/u.

III. NUMERICAL DETAILS

The interelectronic-interaction correction to the differential cross section of radiative recombination of an electron with a He-like ion in the ground state is given by Eq. (16) after a summation over the angular momentum projections μ_v of the final state, over the polarizations of the emitted photon, and averaging over the polarizations μ_i of the incoming electron. Because of the summation over the magnetic substates of the initial and the final states, all physical polarizations of the emitted photon are equivalent. Below we assume that the photon-polarization vector $\boldsymbol{\epsilon}$ has only one spherical component q. The summation over the magnetic substates and the angular integrations are carried out analyti-

cally. As the resulting expressions are rather lengthy, only an outline of the angular reduction technique used here is given in the appendix.

The resulting formulas contain an infinite summation over the Dirac angular-momentum quantum number κ of the incoming electron. In the actual calculations the sum was evaluated until convergence was achieved (typically, up to $|\kappa_{\max}|=10-20$). Another infinite summation is the sum over the intermediate states n in Eqs. (7)–(10). The sum over n for a fixed angular-momentum quantum number κ_n is evaluated using the methods described below. The remaining summation over κ_n is finite after the angular reduction is carried out. The angular reduction yields $\kappa_n=\kappa_v$ for the correction $\tau_1^{\rm int}$ and $\kappa_n=\kappa$ for the correction $\tau_2^{\rm int}$. For the corrections $\tau_3^{\rm int}$ and $\tau_4^{\rm int}$, there are three values of κ_n for each value of κ, which contribute in the case of capture into a state with $j_v=1/2$, and five for $j_v=3/2$.

For the numerical evaluation of the sum over n with a fixed angular-momentum quantum number κ_n, we use different numerical tools. In order to calculate the direct part of the corrections $\tau_1^{\rm int}$ and $\tau_2^{\rm int}$, we solve the Dirac equation with the Coulomb potential modified by the screening potential [Eq (17)]. The difference between the zero-order cross sections evaluated with the modified wave functions and with the Coulomb wave functions can be thought to be the first-order correction induced by the screening potential, plus higher-order ladder contributions. Since the higher-order corrections are suppressed by a factor $1/Z$, the resulting correction can be considered as a good approximation to the corrections $\tau_{1,\rm dir}^{\rm int}$ and $\tau_{2,\rm dir}^{\rm int}$ for high-Z systems (we indicate the direct and the exchange parts with labels ''dir'' and ''exch,'' respectively). For the numerical solution of the Dirac equation with a modified Coulomb potential we use the package RADIAL from Ref. [8], with some minor modifications for continuum solutions.

The numerical evaluation of all other corrections is carried out directly, without any additional approximations. The summation over the whole spectrum of the Dirac equation is performed using two different methods. When the energy argument of the Green function is less than the electron rest mass, we use the B-splines method for the Dirac equation, developed by Johnson *et al.* [9]. In this method, the infinite summation in the spectral representation of the Green function with a fixed angular-momentum quantum number is replaced by a finite sum over basis-set functions. This method is used for the numerical evaluation of the corrections $\tau_{1,\rm exch}^{\rm int}$, $\tau_3^{\rm int}$, and the correction $\tau_4^{\rm int}$ if $\varepsilon_c+k_f^0<m$.

If the energy argument of the Green function is real and larger than the electron rest mass, the B-splines method is not applicable anymore, and we use analytical expressions for the Green function for the potential of a homogeneously charged spherical shell [10]. Numerical algorithms for the computation of the Green function with an extended nucleus can be found in Refs. [11,12]. Special care should be taken evaluating the Green function for real energies larger than the electron rest mass (see, e.g., Ref. [13]). The Green function is an analytical function of the energy ε in the complex ε-plane with branch cuts $(-\infty,-m]$, $[m,\infty)$ along the real ε-axis and poles corresponding to the discrete Dirac energy levels, as shown in Fig. 1. The behavior of the Green function on the real ε axis is defined by the sign of the infinitesimal additions in the energy denominator of Eqs. (8)–(10). In our case the addition is negative and, therefore, the cut $\varepsilon>m$ should be approached from the upper half of the ε-plane. Considering the dependence of the Green function on ε, one can see that the cut structure of the Green function is defined by the branch cuts of the square root $\sqrt{m^2-\varepsilon^2}$. The square root is defined as positive in the gap $-m<\varepsilon<m$ on the real ε-axis. Outside of the gap, the sign of the square root is fixed by the condition $\mathrm{Re}\{\sqrt{m^2-\varepsilon^2}\}>0$. So, starting from the gap $-m<\varepsilon<m$ and approaching the branch cut $\varepsilon>m$ from the upper half-plane, we have $\sqrt{m^2-\varepsilon^2}\to -i\sqrt{\varepsilon^2-m^2}$. This prescription for the analytic continuation of the square root defines the sign of the imaginary part of the Green function.

A numerical evaluation employing the analytical form of the Green function is more time-consuming than a calculation based on the B-splines method. Thus, in actual calculations we used the last method whenever possible. Still, an evaluation of a correction using both methods was used as a check for our code.

IV. NUMERICAL RESULTS AND DISCUSSION

The numerical results for the interelectronic-interaction correction to the total cross section of radiative recombination of an electron with He-like uranium are presented in Table I. The calculations are carried out in the laboratory frame for capture into the $2s$, $2p_{1/2}$, and $2p_{3/2}$ states of He-like uranium and for projectile energies of 10–700 MeV per nuclear mass unit. The various contributions to the cross section listed in Table I correspond to Eqs. (13) and (14); $\sigma_{\rm int}^{(1)}$ denotes the total first-order interelectronic-interaction correction. We note that the correction $\sigma_{1,\rm dir}^{\rm int}+\sigma_{2,\rm dir}^{\rm int}$ contains also some higher-order contributions, which are small compared to the first-order contribution. In Table II we compare the results of the rigorous relativistic treatment for the total cross section with the calculations based on the screening-potential approximation and on the effective-nuclear-charge approximation. A comparison of the corresponding results for the differential cross section is presented in Figs. 3–6. The comparison shows a decreasing accuracy of the approximate methods for increasing projectile energy. They also yield better results for capture into excited states than for capture into the ground state. In average, the screening-potential approximation is found to be more reliable than the effective-nuclear-charge approximation. Its typical deviation from the rigorous treatment is about 10%–20% of the interelectronic-interaction correction, i.e., about 1%–2% of the cross section of the process.

The dominant contribution to the effect of the interelectronic interaction originates from the corrections $\sigma_{\rm en}^{\rm int}$ and $\sigma_{1,\rm dir}^{\rm int}+\sigma_{2,\rm dir}^{\rm int}$, which are almost equivalent to the screening-potential approximation. In addition to this, a significant contribution arises from the correction $\sigma_4^{\rm int}$ in the region of projectile energies $p_i^0<m+\varepsilon_v-\varepsilon_c$. The reason for this is the

TABLE I. Various contributions to the interelectronic-interaction correction to the total cross section for radiative recombination of an electron into lowest-lying states of He-like uranium in barns.

E [Mev/u]	$\sigma^{\rm int}_{\rm en}$	$\sigma^{\rm int}_{1,\rm dir}+\sigma^{\rm int}_{2,\rm dir}$	$\sigma^{\rm int}_{1,\rm exch}$	$\sigma^{\rm int}_{2,\rm exch}$	$\sigma^{\rm int}_{3}$	$\sigma^{\rm int}_{4}$	$\sigma^{(1)}_{\rm int}$
$2s$-state:							
10	−16.162	−3.022	−2.063	1.615	−0.404	−1.357	−21.392
50	−1.984	−1.179	−0.235	0.245	−0.026	−0.548	−3.727
100	−0.664	−0.716	−0.072	0.081	0.005	−0.690	−2.055
200	−0.2009	−0.3738	−0.0206	0.0165	0.0083	−0.112	−0.683
300	−0.0975	−0.2358	−0.0110	0.0038	0.0063	−0.0413	−0.3755
500	−0.0392	−0.1219	−0.0057	−0.0003	0.0039	−0.0131	−0.1764
700	−0.0219	−0.0759	−0.0039	−0.0003	0.0025	−0.0056	−0.1051
$2p_{1/2}$-state:							
10	−31.946	−3.984	1.268	0.574	1.807	−3.115	−35.396
50	−3.465	−2.912	0.334	0.126	0.295	−0.776	−6.398
100	−1.041	−1.560	0.164	0.0614	0.110	−0.821	−3.088
200	−0.2734	−0.6398	0.0683	0.0256	0.0304	0.003	−0.786
300	−0.1208	−0.3435	0.0381	0.0137	0.0116	0.0145	−0.3864
500	−0.0431	−0.1466	0.0173	0.0054	0.0025	0.0083	−0.1562
700	−0.0223	−0.0821	0.0102	0.0027	0.0006	0.0049	−0.0861
$2p_{3/2}$-state:							
10	−35.002	−4.616	1.316	0.496	2.493	−4.695	−40.008
50	−3.061	−3.285	0.250	0.070	0.367	−1.062	−6.721
100	−0.782	−1.523	0.096	0.023	0.126	−0.838	−2.896
200	−0.1679	−0.5238	0.0294	0.0060	0.0330	−0.031	−0.655
300	−0.0649	−0.2523	0.0132	0.0023	0.0130	0.0081	−0.2804
500	−0.0194	−0.0942	0.0045	0.0005	0.0035	0.0080	−0.0970
700	−0.0089	−0.0485	0.0022	0.0001	0.0014	0.0048	−0.0489

smallness of the energy denominator in Eq. (10), which enhances the contribution of the discrete energy states in the sum over the Dirac spectrum. When the energy denominator approaches zero, a resonance occurs that corresponds to the resonance process of dielectronic recombination.

V. CONCLUSION

In this work we have carried out a systematic investigation of the effect of the interelectronic interaction on the process of radiative recombination of an electron with He-like uranium. The applicability of frequently used approximate methods was studied and compared with the rigorous relativistic treatment. The screening-potential approximation, in which an interaction of an electron with a He-like ion is replaced by an interaction with a modified potential, is shown to be a reliable tool for estimating both total and differential cross sections of the process for projectile energies far from resonance. Still, full relativistic calculations are needed to obtain an accuracy better than a few percent of the cross section of the process. The results of the rigorous treatment of the interelectronic-interaction correction are presented for radiative recombination of an electron into $2s$, $2p_{1/2}$, and $2p_{3/2}$ states of He-like uranium for impact energies between 10 and 700 MeV/u.

ACKNOWLEDGMENTS

We want to thank Th. Stöhlker and Prof. E. E. B. Campbell for valuable discussions. Financial support by the DFG (Grant No. 436 RUS 113/479) and by the RFBR (Grant No. 98-02-04111) is gratefully acknowledged. Th. Beier acknowledges also support from the EU-TMR program (contract No. ERB FMRX CT 97-0144).

APPENDIX: ANGULAR INTEGRATION

In this section we briefly describe a technique that was used in this work for angular integrations and summations over magnetic substates in Eqs. (7)–(10). We illustrate this technique, taking the correction $\tau^{\rm int}_3$ as an example. Let us consider the expression

$$K_{3,\rm dir}\equiv\sum_{\mu_c\mu_n}\langle vc|I(k_f^0)|pn\rangle\langle n|\boldsymbol{\alpha}\cdot\boldsymbol{\epsilon}^* e^{-i\mathbf{k}_f\mathbf{x}}|c\rangle, \quad \text{(A1)}$$

originating from the direct part of $\tau^{\rm int}_3$. We expand the wave function $|p\rangle$ of the incoming electron with a defined asymptotic momentum over the wave functions with a defined angular momentum (see Ref. [1] for details[1])

[1]Equations (4.120) and (9.39) of Ref. [1] contain a misprint. An expression $(l+1)\pi/2$ should be added to the phase shift Δ_κ in these equations.

TABLE II. Zeroth-order total cross section $\sigma^{(0)}$ and the first-order interelectronic-interaction correction in different evaluations in barns. $\sigma^{(1)}_{\rm zeff}$ denotes the interelectronic-interaction correction calculated in the effective-nuclear-charge approximation with parameter $Z_{\rm eff}=90.3$, $\sigma^{(1)}_{\rm scr}$ corresponds to the screening-potential approximation, and $\sigma^{(1)}_{\rm int}$ indicates the results of the rigorous relativistic treatment.

E [Mev/u]	$\sigma^{(0)}$	$\sigma^{(1)}_{\rm zeff}$	$\sigma^{(1)}_{\rm scr}$	$\sigma^{(1)}_{\rm int}$
$2s$-state:				
10	504.65	−17.390	−19.635	−21.392
50	93.23	−3.699	−3.207	−3.727
100	41.203	−1.880	−1.393	−2.055
200	16.423	−0.8881	−0.5780	−0.6829
300	9.105	−0.5446	−0.3345	−0.3755
500	4.160	−0.2800	−0.1615	−0.1764
700	2.457	−0.1768	−0.0979	−0.1051
$2p_{1/2}$-state:				
10	656.95	−38.523	−34.978	−35.396
50	92.10	−7.086	−6.204	−6.398
100	33.041	−2.975	−2.535	−3.088
200	10.405	−1.0842	−0.8915	−0.7861
300	5.042	−0.5650	−0.4538	−0.3864
500	1.973	−0.2382	−0.1857	−0.1562
700	1.065	−0.1336	−0.1022	−0.0861
$2p_{3/2}$-state:				
10	854.82	−38.620	−39.671	−40.008
50	100.61	−6.158	−6.278	−6.721
100	31.489	−2.259	−2.275	−2.896
200	8.376	−0.6908	−0.6826	−0.655
300	3.646	−0.3213	−0.3132	−0.2804
500	1.249	−0.1172	−0.1122	−0.0970
700	0.622	−0.0600	−0.0568	−0.0489

$$\psi_{p_i\mu_i(+)}(\mathbf{x})=\frac{1}{\sqrt{p_i^0 p_i}}\sum_{\kappa\mu} i^l e^{i\Delta_\kappa} C^{j\mu}_{lm_l,(1/2)\mu_i} Y^*_{lm_l}(\hat{\mathbf{p}}_i) \times\begin{pmatrix} g_{\varepsilon\kappa}(x)\chi_{\kappa\mu}(\hat{\mathbf{x}}) \\ i f_{\varepsilon\kappa}(x)\chi_{-\kappa\mu}(\hat{\mathbf{x}}) \end{pmatrix}. \quad \text{(A2)}$$

The overall factor in front of the sum corresponds to the normalization of the wave function $\psi_{p_i\mu_i(+)}$ fixed by Eq. (5). $C^{j\mu}_{lm_l,sm_s}$ and $Y_{lm_l}(\hat{\mathbf{p}}_i)$ denote a Clebsch-Gordan coefficient and a spherical harmonic, respectively.

We evaluate the matrix element of the interelectronic-interaction operator by writing it in the form

$$\langle ab|I(\varepsilon)|cd\rangle=\alpha\sum_L J_L(abcd)R_L(\varepsilon,abcd). \quad \text{(A3)}$$

In this way we separate the part depending on angular momentum projections $[J_L(abcd)]$ from the remainder $R_L(\varepsilon,abcd)$, which does not depend on them. The function $J_L(abcd)$ is given by

$$J_L(abcd)=\sum_{m_L}\frac{(-1)^{L-m_L+j_c-m_c+j_d-m_d}}{2L+1} \times C^{Lm_L}_{j_a m_a, j_c-m_c} C^{Lm_L}_{j_d m_d, j_b-m_b}. \quad \text{(A4)}$$

The apparent expressions for the function $R_L(\varepsilon,abcd)$ can be found in Ref. [14].

Now we consider the matrix element of the photon-emission operator $\langle n|\boldsymbol{\alpha}\cdot\boldsymbol{\epsilon}^* e^{-i\mathbf{kx}}|c\rangle$. All terms containing the spherical bispinors $\chi_{\kappa\mu}$ are expanded in terms of the spherical vectors according to

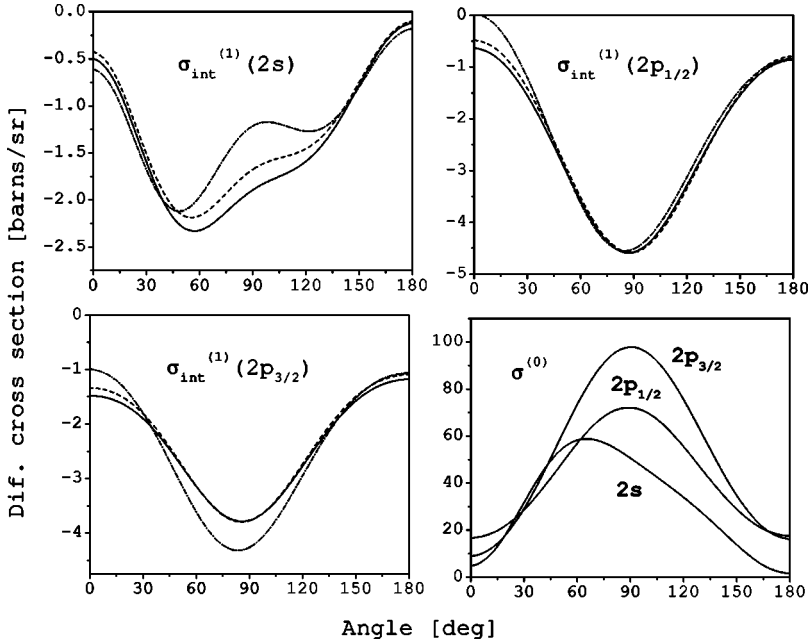

FIG. 3. Interelectronic-interaction correction $\sigma^{(1)}_{\rm int}$ to the differential cross section of radiative recombination into $2s$, $2p_{1/2}$, and $2p_{3/2}$ states of He-like uranium is presented in the first three diagrams. The calculation is carried out in the laboratory system at a projectile energy of 10 MeV/u. The full line refers to the rigorous relativistic treatment. It should be compared with the screening-potential approximation (dashed line) and the effective-nuclear-charge approximation with $Z_{\rm eff}=90.3$ (dashed-dot line). In order to display the relative magnitude of the effect, the zeroth-order differential cross section $\sigma^{(0)}$ is presented in the fourth diagram.

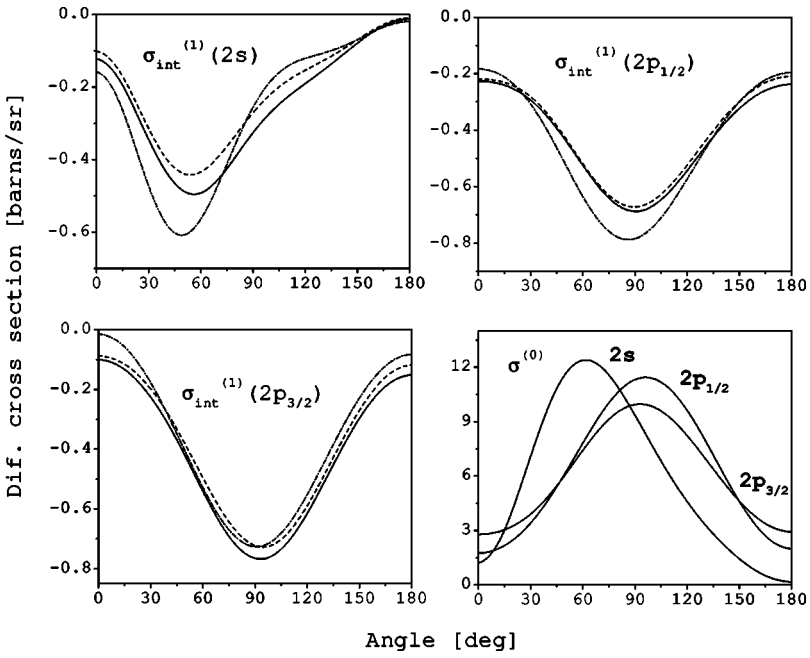

FIG. 4. Same as Fig. 3 but for a projectile energy of 50 MeV/u.

$$\chi^{\dagger}_{\kappa_b\mu_b}(\hat{\mathbf{z}})\boldsymbol{\sigma}\chi_{\kappa_a\mu_a}(\hat{\mathbf{z}}) = \sum_{JLM} \frac{(-1)^{j_b-\mu_b}}{\sqrt{4\pi}} C^{LM}_{j_a\mu_a, j_b-\mu_b} \times S_{JL}(\kappa_b,\kappa_a)\mathbf{Y}_{JLM}(\hat{\mathbf{z}}), \tag{A5}$$

where σ_i are the Pauli matrices, $\mathbf{Y}_{JLM}$ are the spherical vectors defined by

$$\mathbf{Y}_{JLM}(\hat{\mathbf{z}}) = \sum_{mq} C^{JM}_{Lm,1q} Y_{Lm}(\hat{\mathbf{z}})\mathbf{e}_q, \tag{A6}$$

and $\mathbf{e}_q$ are the spherical coordinates of the unit vector. For the apparent expressions for the coefficients S_{JL} we refer to Ref. [14]. Next, we use the standard spherical-waves expansion of the exponent in the photon-emission operator and perform the integration over angular variables. It yields

$$\langle n|\boldsymbol{\alpha}\cdot\boldsymbol{\epsilon}^* e^{-i\mathbf{k}_f\mathbf{x}}|c\rangle = \sum_{JL} i^{-1-L}(-1)^{j_c-\mu_c}\sqrt{2L+1}C^{JM}_{L0,1q} \times C^{JM}_{j_n\mu_n, j_c-\mu_c} P_{JL}(k_f^0, nc). \tag{A7}$$

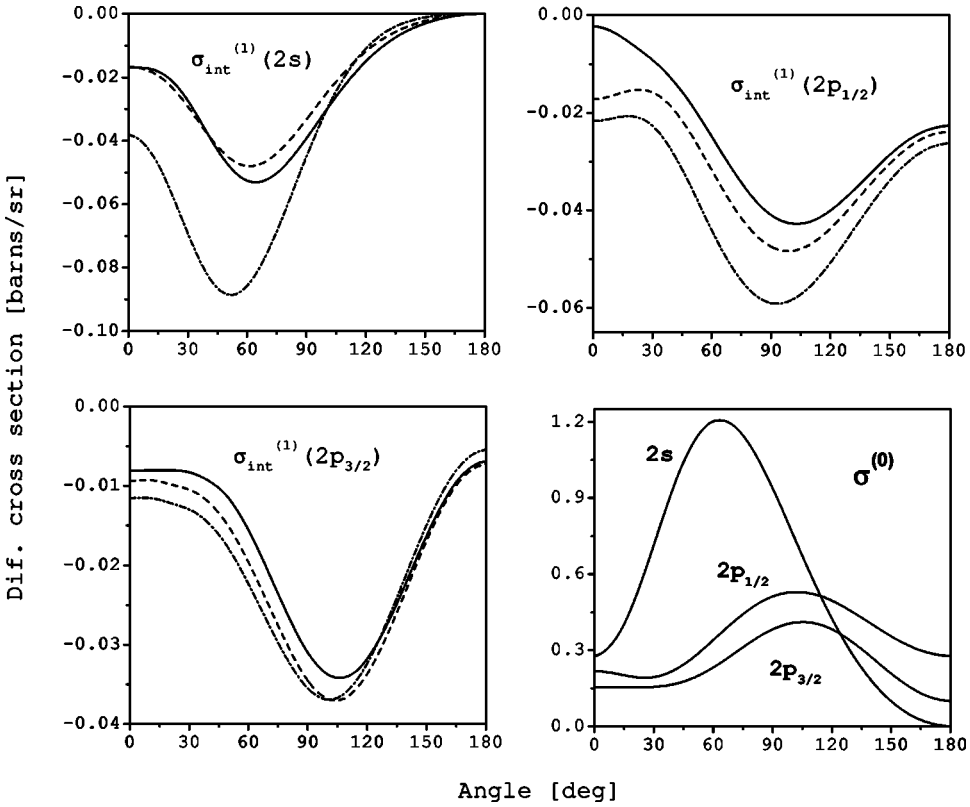

FIG. 5. Same as Fig. 3 but for a projectile energy of 300 MeV/u.

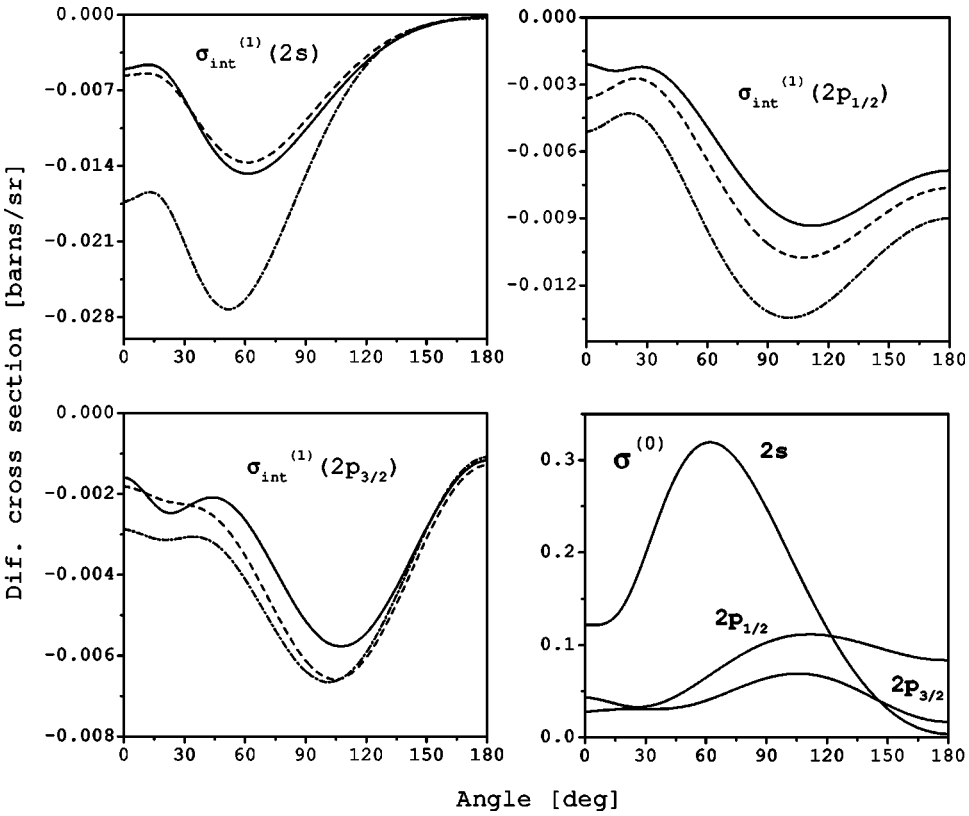

FIG. 6. Same as Fig. 3 but for a projectile energy of 700 MeV/u.

As was explained above, the polarization vector $\boldsymbol{\epsilon}$ has only one spherical component $q=\pm 1$ (nothing depends on its sign). The radial integrals P_{JL} are given by

$$P_{JL}(k_f^0,ab)=\int_0^\infty dx x^2 j_L(k_f^0 x)[g_b(x)f_a(x)S_{JL}(\kappa_b,-\kappa_a) - f_b(x)g_a(x)S_{JL}(-\kappa_b,\kappa_a)], \tag{A8}$$

where $g(x)$ and $f(x)$ are the upper and lower components of the radial wave functions, respectively; $j_L(z)$ is the spherical Bessel function.

Substituting Eqs. (A2), (A3), and (A7) into Eq. (A1) and performing the summation of the Clebsch-Gordan coefficients, we obtain

$$K_{3,\mathrm{dir}}=\frac{1}{\sqrt{p_i^0 p_i}}\sum_\kappa i^l e^{i\Delta_\kappa} C^{j\mu}_{lm_l,(1/2)\mu_i} Y^*_{lm_l}(\hat{\mathbf{p}}_i) \times\sum_{JL} i^{-1-L}(-1)^{j-\mu}\sqrt{2L+1}C^{JM}_{L0,1q}C^{JM}_{j_v\mu_v,j-\mu} \times\frac{\alpha(-1)^{J+j_n-j_c}}{2J+1}R_J(k_f^0,vc\varepsilon n)P_{JL}(k_f^0,nc), \tag{A9}$$

where $|\varepsilon\rangle$ denotes the radial wave function of the incoming electron with a definite angular momentum

$$|\varepsilon\rangle=\begin{pmatrix} g_{\varepsilon\kappa}(x) \\ f_{\varepsilon\kappa}(x)\end{pmatrix}. \tag{A10}$$

Finally, we have for the τ_3^{int} correction

$$\tau_3^{\mathrm{int}}=\frac{\alpha}{\sqrt{2(2\pi)^3 k_f^0 p_i^0 p_i}}\sum_\kappa i^l e^{i\Delta_\kappa} C^{j\mu}_{lm_l,(1/2)\mu_i} Y^*_{lm_l}(\hat{\mathbf{p}}_i) \times\sum_{JL} i^{-1-L}(-1)^{j-\mu}\sqrt{2L+1}C^{JM}_{L0,1q}C^{JM}_{j_v\mu_v,j-\mu} \times\sum_{\kappa_n}(-1)^{j_c-j_n+J}[\mathcal{R}^{\mathrm{int}}_{3,a}(J,L,k_f^0)S_{JL}(\kappa_c,-\kappa_n) - \mathcal{R}^{\mathrm{int}}_{3,b}(J,L,k_f^0)S_{JL}(-\kappa_c,\kappa_n)], \tag{A11}$$

where

$$\mathcal{R}^{\mathrm{int}}_{3,i}(J,L,k_f^0)=\frac{1}{2J+1}R_J(k_f^0,vc\varepsilon\xi_i)-\sum_{L'}\begin{Bmatrix} j_c & j_n & J \\ j_v & j & L'\end{Bmatrix} \times R_{L'}(p_i^0-\varepsilon_c,cv\varepsilon\xi_i), \tag{A12}$$

and the effective wave function $\xi_i(y)$ is given by

$$|\xi_a\rangle=\sum_n\frac{|n\rangle}{\varepsilon_c-k_f^0-\varepsilon_n(1-i0)}\int_0^\infty dx x^2 j_L(k_f^0 x)f_n(x)g_c(x), \tag{A13}$$

$$|\xi_b\rangle=\sum_n\frac{|n\rangle}{\varepsilon_c-k_f^0-\varepsilon_n(1-i0)}\int_0^\infty dx x^2 j_L(k_f^0 x)g_n(x)f_c(x). \tag{A14}$$

[1] J. Eichler and W. Meyerhof, *Relativistic Atomic Collisions* (Academic Press, San Diego, 1995).

[2] A. Ichihara, T. Shirai, and J. Eichler, Phys. Rev. A **49**, 1875 (1994); J. Eichler, A. Ichihara, and T. Shirai, *ibid.* **51**, 3027 (1995).

[3] Th. Stöhlker, T. Ludziejewski, F. Bosch, R.W. Dunford, C. Kozhuharov, P.H. Mokler, H.F. Beyer, O. Brinzanescu, F. Franzke, J. Eichler, A. Griegal, S. Hagmann, A. Ichihara, A. Krämer, D. Liesen, H. Reich, P. Rymuza, Z. Stachura, M. Steck, P. Swiat, and A. Warczak, Phys. Rev. Lett. **82**, 3232 (1999).

[4] Th. Stöhlker, H. Geissel, H. Irnich, T. Kandler, C. Kozhuharov, P.H. Mokler, X. Münzenberg, F. Nickel, C. Scheidenberger, T. Suzuki, M. Kucharski, A. Warczak, P. Rymuza, Z. Stachura, A. Kriessbach, D. Dauvergne, B. Dunford, J. Eichler, A. Ichichara, and T. Shirai, Phys. Rev. Lett. **73**, 3520 (1994).

[5] V.M. Shabaev, Phys. Rev. A **50**, 4521 (1994).

[6] V.M. Shabaev, V.A. Yerokhin, T. Beier, and J. Eichler, Phys. Rev. A **61**, 052112 (2000).

[7] M.A. Braun, A.D. Gurchemelija, and U.I. Safronova, *Relativistic Atomic Theory* (Nauka, Moscow, 1984) [in Russian]; M.B. Shabaeva and V.M. Shabaev, Phys. Rev. A **52**, 2811 (1995).

[8] F. Salvat, J.M. Fernańdez-Varea, and W. Williamson, Jr., Comput. Phys. Commun. **90**, 151 (1995).

[9] W.R. Johnson, S.A. Blundell, and J. Sapirstein, Phys. Rev. A **37**, 307 (1988).

[10] M. Gyulassy, Nucl. Phys. A **244**, 497 (1975).

[11] G. Soff and P.J. Mohr, Phys. Rev. A **38**, 5066 (1988).

[12] P.J. Mohr, G. Plunien, and G. Soff, Phys. Rep. **293**, 227 (1998).

[13] L.D. Landau and E.M. Lifshitz, *Quantum Mechanics* (Pergamon Press, Oxford, 1977).

[14] V.A. Yerokhin and V.M. Shabaev, Phys. Rev. A **60**, 800 (1999).